



**HAL**  
open science

## Rainfall Estimation in the Sahel. Part I: Error Function

Abdou Ali, Thierry Lebel, Abou Amani

► **To cite this version:**

Abdou Ali, Thierry Lebel, Abou Amani. Rainfall Estimation in the Sahel. Part I: Error Function. Journal of Applied Meteorology, 2005, 44 (11), pp.1691 à 1706. 10.1175/JAM2304.1 . insu-00382039

**HAL Id: insu-00382039**

**<https://insu.hal.science/insu-00382039>**

Submitted on 19 Feb 2021

**HAL** is a multi-disciplinary open access archive for the deposit and dissemination of scientific research documents, whether they are published or not. The documents may come from teaching and research institutions in France or abroad, or from public or private research centers.

L'archive ouverte pluridisciplinaire **HAL**, est destinée au dépôt et à la diffusion de documents scientifiques de niveau recherche, publiés ou non, émanant des établissements d'enseignement et de recherche français ou étrangers, des laboratoires publics ou privés.

## Rainfall Estimation in the Sahel. Part I: Error Function

ABDOU ALI

*IRD, LTHE, Grenoble, France, and Centre AGRHYMET, Niamey, Niger*

THIERRY LABEL

*IRD, LTHE, Grenoble, France*

ABOU AMANI

*Centre AGRHYMET, Niamey, Niger*

(Manuscript received 29 June 2004, in final form 2 June 2005)

### ABSTRACT

Rainfall estimation in semiarid regions remains a challenging issue because it displays great spatial and temporal variability and networks available for monitoring are often of low density. This is especially the case in the Sahel, a region of 3 million km<sup>2</sup> where the life of populations is still heavily dependent on rain for agriculture. Whatever the data and sensors available for rainfall estimation—including satellite IR and microwave data and possibly weather radar systems—it is necessary to define objective error functions to be used in comparing various rainfall products. This first of two papers presents a theoretical framework for the development of such an error function and the optimization of its parameters for the Sahel. A range of time scales—from rain event to annual—are considered, using two datasets covering two different spatial scales. The mesoscale [Estimation des Pluies par Satellite (EPSAT)-Niger (E-N)] is documented over a period of 13 yr (1990–2002) on an area of 16 000 km<sup>2</sup> covered by 30 recording rain gauges; the regional scale is documented by the Centre Regional Agrometeorologie–Hydrologie–Météorologie (AGRHYMET) (CRA) dataset, with an annual average of between 600 and 650 rain gauges available over a period of 8 yr. The data analysis showed that the spatial structure of the Sahelian rain fields is markedly anisotropic, nonstationary, and dominated by the nesting of two elementary structures. A cross-validation procedure on point rainfall values leads to the identification of an optimal interpolation algorithm. Using the error variances computed from this algorithm on 1° × 1° and 2.5° × 2.5° cells, an error function is derived, allowing the calculation of standard errors of estimation for the region. Typical standard errors for monthly rainfall estimation are 11% (10%) for a 10-station network on a 2.5° × 2.5° (1° × 1°) grid, and 40% (30%) for a single station on a 2.5° × 2.5° (1° × 1°) grid. In a companion paper, this error function is used to investigate the differences between satellite rainfall products and how they compare with ground-based estimates.

### 1. Introduction

The possible long-term modification of the Sahelian precipitation regime (e.g., Lebel et al. 2003) makes hydrologists and climatologists ask themselves two major types of questions: 1) How and to what degree of accuracy can Sahelian rainfall be monitored in real or near-real time to meet the needs of a large community of users faced with the effects of persistent drought (seasonal crop monitoring, water resource manage-

ment, food aid programs)? 2) How and to what degree of significance can the interannual fluctuations of Sahelian rain fields and possible modifications of the precipitation regime be characterized? Considering the deterioration of rain gauge networks (Fig. 1), data access problems, and the significant variability in time and space of Sahelian rainfall, satellite estimates are looked to as a substitute for—or complement of—ground-based network estimates, particularly as satellite-borne sensors become increasingly efficient. This problem is not specific to the Sahel: the past decade has seen the development of rain products intended for a large community of users aiming to summarize as well as possible the information from ground-based networks and sat-

---

*Corresponding author address:* Abdou Ali, B.P. 11416, IRD, Niamey, Niger.  
E-mail: a.ali@agrhytmet.ne

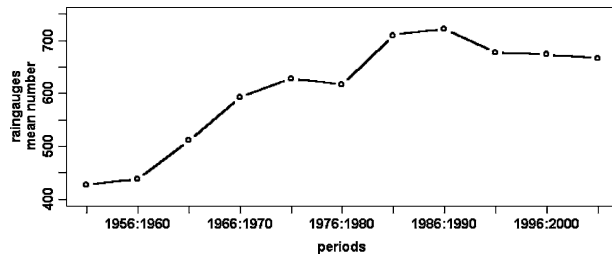


FIG. 1. Evolution of the mean number of CILSS network gauges providing monthly values (averages over 5-yr periods) between 1950 and 2002. After a maximum of over 700 stations at the end of the 1980s, the average number of monthly values has decreased over the past 15 yr.

ellites for a given region. Monitoring rainfall performance is nevertheless a particularly sensitive issue in the Sahel.

The vulnerability of West Africa to the drought that has been prevailing since the 1970s has resulted in the creation of regional institutions to manage better its effects. The Agrometeorologie–Hydrologie–Météorologie (AGRHYMET) Regional Center (CRA), based in Niamey, Niger, is one of the major bodies among them and currently uses many tools for operational activities: systems for early warning, resource water management, and hydrological and agronomic monitoring. Areal rainfall is the main input data for these tools. Whatever the sources of information and procedure used for estimating this rainfall are, the associated error is seldom evaluated with rigor and is less often used in the models.

This work aims at developing an objective method for evaluating the quality of rainfall estimates over the region. The emphasis is on the determination of an error function, inferred from analysis of several years of data—years that can be considered to be representative of the region’s current climate—and analysis on a range of scales meeting the needs of a large community of users. The requirements to be met by a climatological product are different enough from those of products that will be described here as “hydrological,” in the sense that they should especially serve as input data for water balance or water resource quantification models. Yet, it is intuitive that—as is clearly shown in this study—the errors depend heavily on rain field variability, and this variability is far from being consistent from one year to the next. Moreover, this variability naturally depends on the time scale on which our work is based.

Thus, this series of two articles deals with two closely related issues. The first, which is the subject of this article, consists of determining an error function used 1) to develop reference rain fields by minimizing this function and 2) to provide criteria for the intercompari-

son of various rain products. The second issue is addressed in a companion paper and relates to the intercomparison of various rain products while focusing more on error distributions than on mean values.

The main objective of this paper is thus to provide a general framework for users who need to build or to evaluate rain products. In this respect, the results are felt to extend beyond the Sahelian region itself and to apply to most semiarid regions of the intertropical belt. Great care is paid to account for all of the information provided by various sources of rain gauge data, whether from operational origins or research origins. Using the wide conceptual possibilities of geostatistics, a refined characterization of the Sahelian rain fields is used to compare several estimation methods. This, in turn, proposes a coherent interpolation approach and an operational set of metrics for the evaluation of rain products that are presented in the companion paper.

Section 2 briefly reviews the general question of rainfall estimation and the methods available for a quantitative evaluation of the errors associated with any estimation procedure. The application of these methods to the interpolation of Sahelian rain fields (characterized by a strong intermittency in time and space) is then the object of section 3. Section 4 presents a comparison of results between different formulations of kriging, showing that the nonstationarity and anisotropy of the Sahelian rain fields heavily influence the performance of these methods. This result leads, in section 5, to the derivation of an error function associated with the choice of an optimal model of covariance. Conclusions are in section 6.

## 2. Rainfall estimation from ground data

### a. General framework

For the problem treated here, stochastic interpolation methods are the most relevant, because they provide an error evaluation of the estimation made. Apart from some empirical–statistical studies (e.g., Huff 1970; Rudolf et al. 1994; Huffman 1997), almost the entire group of statistical methods refers more or less to the concept of optimal interpolation, initially promoted by Gandin (1965). Matheron’s (1971) theory of regionalized variables expands the framework of optimal interpolation by taking into account the uncertainties related to sampling over a necessarily limited area. As a matter of fact, the empirical mean and spatial variance (i.e., inferred from data) may be highly biased estimators of the mean and variance of the process. Geostatistical methods are widely recognized as performing better than conventional methods (Creutin and Obled 1982; Boussières and Hogg 1989; Philips et al. 1992;

Zimmerman et al. 1999). This fact is particularly true with anisotropic data, as shown by Collins and Bolstad (1996) in comparing kriging with the inverse-distance method.

Very often, the choice of an interpolation method is not so much a question of interpolation per se but rather is a question of evaluating as precisely as possible the errors associated with the interpolation procedure. Geostatistical methods are deemed *optimal*, in the sense that they seek to minimize an error function derived from a representation of the spatial covariance function of the process being studied, with rainfall treated as a bidimensional random process  $P$ . This error function is the variance of estimation error. It should be noted that because rain fields are not linear, nonlinear kriging (Matheron 1976; Journel 1983; Rivoirard 1994; Chica-Olmo and Luque-Espinar 2002) could improve the quantification of the estimation variance. However, nonlinear kriging has its own inconveniences. Nonlinear methods require assumptions for which no methods of verification are currently available, and they can yield solutions that are computationally complex (Cressie 1993; Huang et al. 2002). Also, the mathematical rationale underlying the indicator kriging is flawed, as mentioned by Moyeed and Papritz (2002), which explains why linear kriging remains a good compromise between the search for optimality and the requirements of simplicity.

*b. Structural analysis and inference of the space covariance function*

To filter out any bias in the estimation of the mean and variance of the random process under consideration, its spatial structure is represented by the variogram, defined as

$$\gamma(x_1, x_2) = (1/2) \text{Var}[P(x_1) - P(x_2)], \tag{1}$$

where  $x_1$  and  $x_2$  are two points in the 2D space.

Nonstationarity (e.g., Sampson and Guttorp 1992) and anisotropy (Ecker and Gelfand 2003) may imply that the field variance and/or the decorrelation distance change according to the directions considered. They are thus two important factors to take into account in the inference process.

To infer the mean structure of the rainfall process, a mean variogram (Guillot and Lebel 1999; Furrer 2002) will be computed as follows:

$$\begin{aligned} \gamma_m^*(x_1, x_2) &= \frac{1}{2K} \left\{ \sum_{k=1}^K [P(x_{1k}) - P(x_{2k})]^2 \right\} \\ &\quad - \frac{1}{2K^2} \left\{ \sum_{k=1}^K [P(x_{1k}) - P(x_{2k})] \right\}^2, \tag{2} \end{aligned}$$

where  $x_1$  and  $x_2 \in \mathfrak{R}^2$  and  $K$  is the number of rain events.

For large time steps (e.g., month), because of the nonhomogeneity of the rain fields and the presence of a drift (Ali et al. 2003), the variogram considered is the mean variogram of the residual  $\varepsilon^*$ . The model used for the interpolation is obtained by grouping the  $K \times N$  available data ( $N$  is number of stations) into distance classes:

$$\begin{aligned} \gamma_m^*(h) &= \gamma_m^*(h) \\ &= \frac{1}{K} \sum_{k=1}^K \left\langle \frac{1}{2n} \left\{ \sum_{i,j=1}^n [\varepsilon^*(x_{ik}) - \varepsilon^*(x_{jk})]^2 \right\} \right\rangle, \tag{3} \end{aligned}$$

where  $n$  is the number of couples of points  $x_i$  and  $x_j$  separated by distance  $h \pm \Delta h$ .

*c. Kriging estimators*

Consider

$$P_S = \frac{1}{S} \int_S P(x) d(x), \tag{4}$$

where  $P_S$  is the areal rainfall to estimate over a given domain  $S$ , with  $x$  being a point in the 2D space. Based on the available measurements at  $N$  stations located in  $x_i$ , the linear estimator is

$$P_S^* = \sum_{i=1}^N \lambda_i P(x_i). \tag{5}$$

Linear estimators are distinct from each other in the way they compute the weighting coefficients  $\lambda_i$ . In kriging, the weighting coefficients are computed in such a way that the estimate is unbiased:

$$E(P_S^* - P_S) = 0 \tag{6a}$$

and its variance (the kriging variance) is minimized:

$$\min[\text{Var}(P_S^* - P_S)]. \tag{6b}$$

Whereas at small time scales rain fields may be treated as a purely stochastic process, at larger time scales (daily and over) a deterministic component— $m(x)$ —may be present (linked to the topography or any other geographical forcing factor) along with a stochastic component— $\varepsilon(x)$ :

$$P(x) = m(x) + \varepsilon(x). \tag{7}$$

The stochastic component is assumed to be second-order stationary and  $E[\varepsilon(x)] = 0$ . The various formulations of kriging depend on the nature of  $m(x)$ .

If  $m(x)$  is constant and known, the kriging formula-

tion is called simple kriging (SK); if it is constant but unknown, the kriging formulation is called ordinary kriging (OK). One can refer to Cressie (1993) and Chilès and Delfiner (1999), for example, for a full presentation of these methods. The kriging variances of estimation error at point  $x_0$  for SK and OK are

$$\sigma_{\text{SK}}^2 = \sum_{i=1}^N \lambda_{\text{SK}_i} \gamma_{\varepsilon}(x_i, x_0) \quad \text{and} \quad (8)$$

$$\sigma_{\text{OK}}^2 = \sum_{i=1}^N \lambda_{\text{OK}_i} \gamma_{\varepsilon}(x_i, x_0) + \mu_{\text{OK}}, \quad (9)$$

where  $\gamma_{\varepsilon}$  is the variogram of the underlying process  $\varepsilon$ , which in this case is also the variogram of  $P$ ;  $\mu_{\text{OK}}$  is the Lagrange multiplier accounting for the constraint on the weights of the OK system.

If  $m(x)$  depends on the 2D coordinates  $x$ , nonstationary geostatistical methods must be considered (Matheron 1969). Two methods, universal kriging and regression kriging, are tested<sup>1</sup> here.

Universal kriging (UK) was first formulated by Matheron (1969), was further developed by several authors (Journal and Huijbregts 1978; Papritz and Stein 1999), and is based on a global resolution of the kriging system, assuming a polynomial form for the drift, that is to say:

$$m(x) = \sum a_l f^l(x). \quad (10)$$

The estimation variance of the UK is obtained as follows:

$$\sigma_{\text{UK}}^2 = \sum_{i=1, N} \lambda_{\text{UK}}^i \gamma_{\varepsilon}(x_i, x_0) + \sum_l \mu_{\text{UK}^l} \times f^l(x_0). \quad (11)$$

In the UK system the variogram  $\gamma_{\varepsilon}$  of the underlying process  $\varepsilon$  is not known in practice, because the coefficients of the drift  $[m(x)]$  model are not known. Several authors (Cressie 1993; Goovaerts 1997; Chilès and Delfiner 1999) draw attention to the biased behavior of the variogram used in the universal kriging system.

The second approach, in the case of nonstationarity, is regression kriging (RK; Ahmed and de Marsily 1987; Odeh et al. 1995; Goovaerts 1997). Here the predictions are made separately for the drift and the residuals and then are added back together. The method consists of three steps: 1) subtracting the drift values  $[m(x_i)]$  from

the observations  $[P(x_i)]$ , 2) kriging the obtained residuals  $[\varepsilon^*(x_i)]$ , and 3), for each point  $x_0$  for which an estimation is sought, combining the estimated value of the drift  $\hat{m}(x_0)$  to the kriged residual  $\hat{\varepsilon}(x_0)$ :

$$\hat{P}_{\text{RK}}(x_0) = \hat{m}(x_0) + \hat{\varepsilon}(x_0). \quad (12)$$

The drift model coefficients are optimally estimated using the generalized least squares so as to account for the spatial correlation of residuals (Cressie 1993; Hengl et al. 2003). This idea resolves the problem mentioned for UK, because only the variogram of the residuals is required, which can be estimated from the experimental residuals. However, the experimental residuals contain the drift estimation error, which produces a nugget effect on the residual variogram:

$$\hat{\gamma}_{\text{RK}} = \gamma_{\varepsilon} + \sigma_m^2, \quad (13)$$

where  $\sigma_m^2$  is the regression error variance, assumed to be stationary over the study area.

In numerical terms, residual kriging is thus comparable to kriging data affected by a measurement error. The residual kriging variance represents the global error associated with the estimation by the RK system, that is, the sum of two errors—one linked to the regression estimation and the other to the undersampling of the underlying process  $\varepsilon$ :

$$\sigma_{\text{RK}}^2(x_0) = \sigma^2[\hat{m}(x_0)] + \sigma^2[\hat{\varepsilon}(x_0)], \quad (14)$$

where  $\sigma^2[\hat{m}(x_0)]$  is the regression variance error and  $\sigma^2[\hat{\varepsilon}(x_0)]$  is the kriging variance of the stochastic process component due to the sampling.

It is important to specify that whichever kriging method is used, the estimation error does not depend on an eventual bias of the point measurements. Also, as can be noted from above, all of the kriging variances are expressed from the variogram and the drift, which implies the importance of inferring them properly.

### 3. Structural analysis of the Sahelian rain fields and scale considerations

#### a. Data used for calibration and validation

The data used in this work come from two networks covering two different scales. One is the Estimation des Pluies par Satellite (EPSAT)-Niger (E-N) mesoscale network, described in D'Amato and Lebel (1998). This network covers an area of 16 000 km<sup>2</sup> in the region of Niamey, Niger (Fig. 2a), and has been in operation since 1990. It consists of digitized recording rain gauges providing time series of 5-min rainfall at 30 stations. From 1990 to 1993, a greater number of stations (107 stations in 1992 and 1993) were available, which, be-

<sup>1</sup> Note that only the univariate form of kriging is considered here because the Sahel is a fairly flat region and no direct relation between vegetation and rainfall is known; bivariate kriging, such as cokriging (Wackernagel 1998), may be more suitable in other contexts.

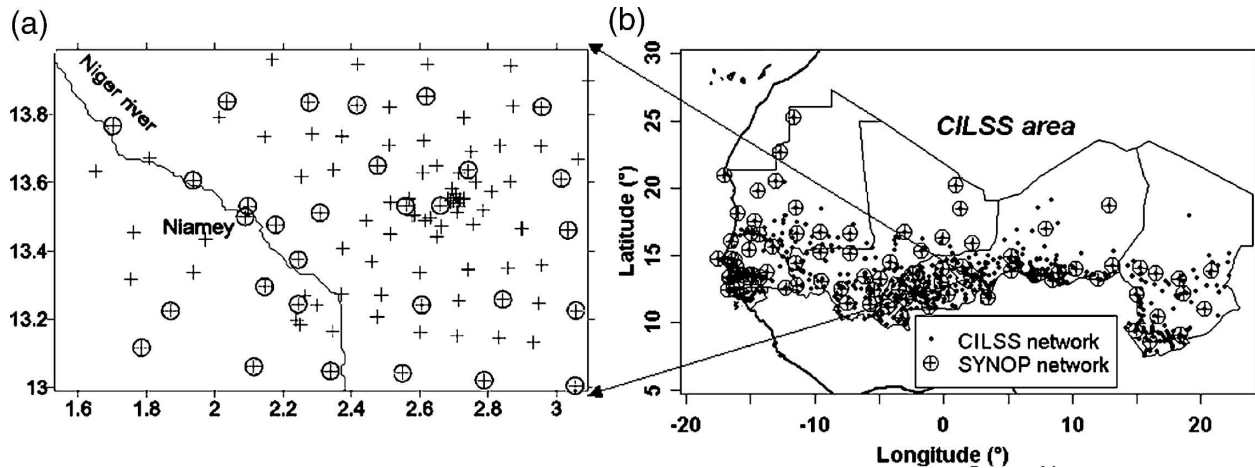


FIG. 2. (a) Mesoscale: the EPSAT-Niger network is made of recording rain gauges covering  $16\,000\text{ km}^2$ , with a denser network (+) of 107 stations (1990–93) and a long-term network (circles) of 30 stations (1990–2003). (b) Regional scale: the CILSS dataset in 2000 covering approximately  $3 \times 10^6\text{ km}^2$ , with 680 daily reading rain gauges; also shown is the synoptic network, which includes 87 stations.

cause of a nested pattern, allowed for a characterization of the spatial structure of the rain fields at a 1-km resolution. The data from the 1990–2002 period are used here. They correspond to a total of 548 rain events, associated with mesoscale convective systems. These rain events represent 90% of the total rainfall over the area covered by the network. This dataset was mainly used for the identification of the structure function at small spatial scales and for validation on very dense networks.

The second dataset used here comes from CRA. It was used for both calibration and validation (using a cross-validation procedure) at the regional scale. This database includes the daily rain data collected by the national rain gauge networks of the Comité Inter-Etats de Lutte Contre la Sécheresse au Sahel (CILSS) countries. These networks cover more than 3 million  $\text{km}^2$  and total more than 1200 stations. There are, however, significant fluctuations in the number of stations providing data each year. Over the period of 1990–2000 there are less than 800 stations available each year. At the daily scale, a consistent dataset of 8 yr (1990, 1992, 1994, and 1996–2000) was retained: 914 stations have at least 1 yr of data over the period of 1990–2000, the minimum number of gauges is 704 (for 1990 and 2000) and the maximum is 760 (for 1997 and 1999, and 427 stations have full data for the entire period. At the monthly scale, there must be less than 10% of missing daily data to keep the station. For larger time scales (10 days and more), all years of the 1990–2002 period were used. The localization of this network (hereinafter referred to as the “CILSS” network) and its pattern for the year 2000 are shown in Fig. 2b.

The E-N network allows the computation of areal

rainfall over areas ranging from 1000 to 10 000  $\text{km}^2$ , with an average error of less than 5% at the monthly scale and 10% at the event scale (Lebel and Amani 1999). In particular, this allows an objective definition of rain events, which makes the calibration of some integrated approaches in modeling Sahelian rain fields possible, because the number of events is the major factor of rain-field variability.

The CILSS network provides relatively good coverage at the regional scale with an average density of one station per 3500  $\text{km}^2$  (in comparison with one station per 400  $\text{km}^2$  of the E-N network); however, the stations are unevenly distributed. Although the number of rain gauges is, on average, 15 gauges per  $2.5^\circ \times 2.5^\circ$ , 5% of the  $2.5^\circ \times 2.5^\circ$  cells are without any gauge and 30% of the  $1^\circ \times 1^\circ$  cells are without any gauge. This situation (medium density and uneven distribution of stations) is atypical of cases in which optimal interpolation performs better than other methods (e.g., Delhomme 1978; Lebel et al. 1987).

#### b. The Sahelian rain fields and scale-related considerations

There are three important characteristics of the Sahelian rain fields to consider for interpolation purposes. The first is the existence of a strong intermittency in space, linked to the convective nature of rain in the region; it involves a significant spatial variability at all time scales. At the rain-event scale, D’Amato and Lebel (1998) have estimated the intermittency in space to be 0.26, which means that, on average, over an area of  $1^\circ \times 1^\circ$ , 26% of the surface area is not touched by rain. A second important factor is that the rainfall process may be considered stationary at the event scale,

whereas at higher time scales, the process is nonstationary, with the mean and variance presenting a north-south and east-west drift. The third characteristic to consider is the existence of two anisotropic directions: an east-west direction associated with the dominant direction of movement of convective systems and a north-south direction associated with the number of events, with the probability of occurrence being greater in the south than in the north. Depending on the time scale considered, one direction of anisotropy has a greater effect than the other.

### c. Structural analysis

#### 1) MESOSCALE

The characterization of the spatial structure of Sahelian rain fields at the event scale for distances smaller than 150 km is based on the E-N dataset. Over an area of 16 000 km<sup>2</sup>, the mean of the spatial variance of the events is 120 mm<sup>2</sup>, whereas the point variance computed on the 548 rain events is 205 mm<sup>2</sup>. It is obvious that the area covered is too small for the integral variance to reach the variance of the process as confirmed when analyzing the daily CILSS data (daily rain fields have a structure comparable to that of the event rain fields), showing a decorrelation range of 1000 km in the east-west direction. This situation led Guillot and Lebel (1999) to propose a nested variogram, which is the only way to account for both the mesoscale structure and the regional structure of the rain process. This model was fitted to the E-N data by Ali et al. (2003), using two anisotropic exponential functions with an anisotropy coefficient of 1/2 for the first structure and 1/3 for the second structure. At larger time scales (10-day to seasonal), the nonstationarity of the rain fields requires one to infer separately a drift and the variogram of the residuals to this drift (see appendix A for details).

#### 2) REGIONAL SCALE

The CILSS data are used to analyze the spatial structure at larger distances and for time steps ranging from the daily to seasonal scale. To verify that the modeling of the event rain-field structure carried out with the E-N data alone was reasonably extrapolated for distances larger than 150 km, a comparison of the daily variograms obtained from the E-N data, on the one hand, and from the CILSS data, on the other hand, was made (see Fig. 3a).

The decorrelation distance of the CILSS daily variogram is larger than 1000 km, with a spatial variance of 150 mm<sup>2</sup>. The point variance of the daily E-N data is 180 mm<sup>2</sup>. The CILSS variogram displays an anisotropy

comparable to that of the E-N variogram. Accounting for the differences in sampling and of the sensors, the CILSS data and the E-N data provide a coherent picture of the variability of the daily rain fields. The difference between the spatial variance and the point variance is likely to be linked to the assumption of a homogeneous population of rain events not being fully verified, thus adding some variance in the interevent dimension. The daily variogram is represented by a model similar to the one used for the event variogram, with identical parameters for the decorrelation distance and anisotropy of the first structure, and a larger range and stronger anisotropy of the second structure at the daily scale.

At the monthly scale, the raw variograms (whether computed as the mean or as the climatological case) are highly biased by the drift. When subtracting only the north-south drift, the east-west residual variogram still displays a drift, even though somewhat smaller. This fact allows the identification of an east-west drift. Subtracting both the north-south and the east-west drifts produces a mean variogram devoid of any apparent drift, as can be seen in Fig. 3b. The mean monthly drift (correlation coefficient = 0.97) is the following:

$$m(x, y) = -0.75y^2 - 9.62y - 2.44x + 412, \quad (15)$$

where  $x$  and  $y$  are the longitude and the latitude coordinates, respectively, in degrees and  $m$  is in millimeters.

The decorrelation distance of the monthly residual variogram is of the same order as that of the event residual variogram (more than 1000 km) and is also strongly anisotropic (1/3). An important point to underline is that, from the daily scale to the seasonal scale, the raw variograms are biased by the north-south and east-west drifts. This drift is, in fact, a function of the number of rainy days, as shown in Fig. 4. Therefore, RK is a good candidate for interpolating these fields.

### d. A model of spatial structure based on scale considerations

Ali et al. (2003) have developed a scale-invariant formulation of the structure function used for kriging interpolation. This formulation uses the structure function of the event rain fields as the kernel from which the structure functions at larger time scales are derived. This approach avoids the computation of a specific variogram for each time step of interest and guarantees the overall coherence of the structure functions over a broad spectrum of time scales. Rather than identifying an average variogram for the 10-day or monthly rainfall, for instance, rain fields are treated as the accumulation of  $N$  event rain fields, characterized by an  $N$ -event variogram. The scaling procedure is based on the

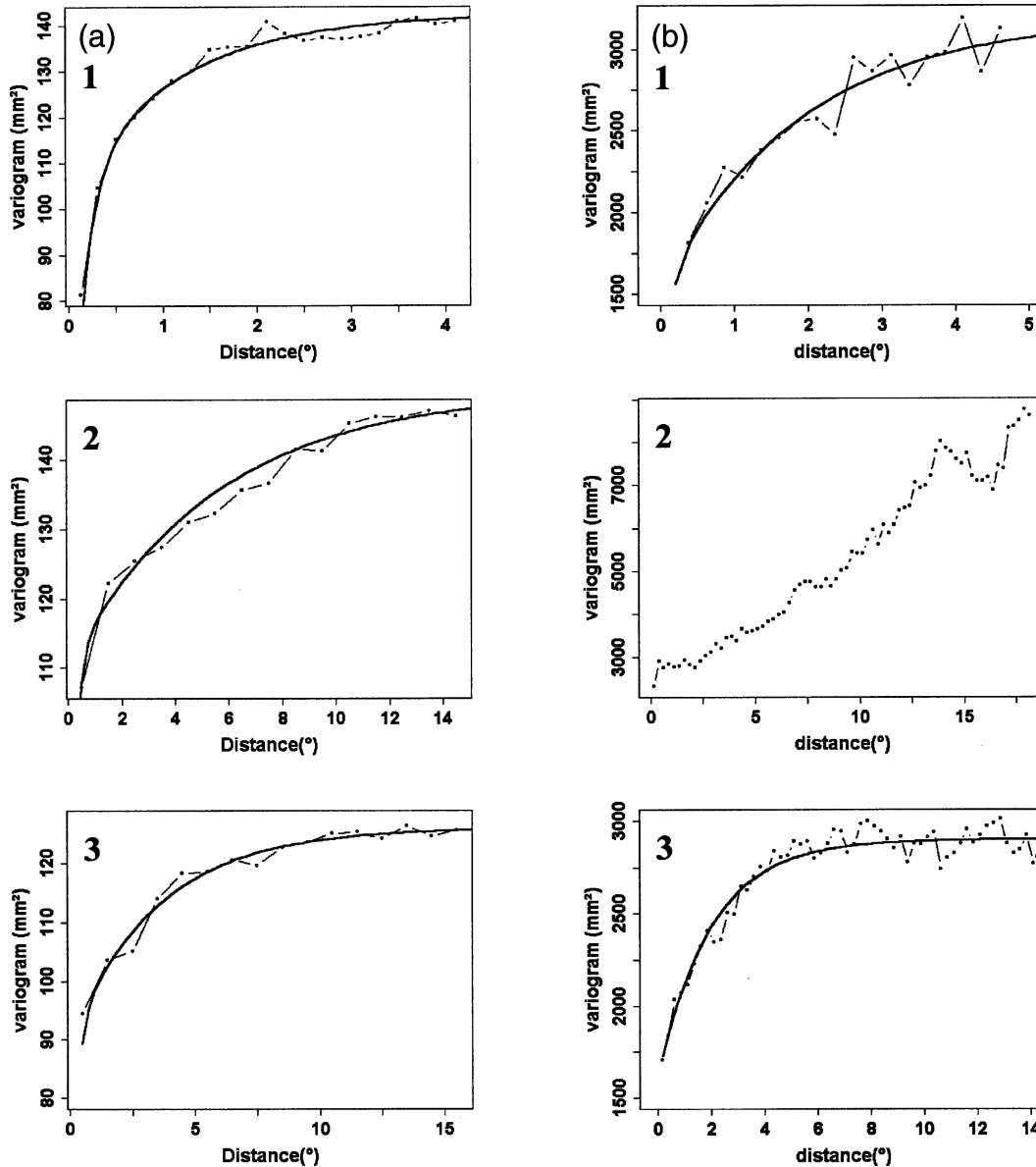


FIG. 3. Variograms computed from (a) 8 yr of the CILSS dataset for daily rainfall and (b) 13 yr (1990–2002) for monthly rainfall. (a1) Mean east–west (E–W) variogram; (a2) mean south–north (S–N) variogram; (a3) residual variogram of the daily rain field in the E–W direction. (b2) Mean monthly E–W variogram with only the S–N drift subtracted. In (b1) (S–N variogram) and (b3) (E–W variogram), the drift is subtracted both in the E–W and S–N directions. We can note a high anisotropy between the E–W (decorrelation distance  $> 10^\circ$ ) and the N–S (decorrelation distance  $\approx 4^\circ$ ) variogram for both the daily and the monthly scale.

analysis of the field of the number of events  $N(x)$ , the spatial structure of which may be represented through the variogram of the indicator function  $I: I_k(x) = 0$  if no rainfall is recorded at point  $x$  for event  $k$ , and  $I_k(x) = 1$  if rainfall is recorded at point  $x$  for event  $k$ . Scale-invariant kriging will be considered here as a possible alternative to traditional OK, UK, or RK, so as to obtain an optimal error function.

#### 4. Optimal interpolation of the Sahelian rain fields

##### a. Possible interpolation functions

Five formulations of kriging are considered in what follows for selecting an optimal interpolation function of Sahelian rain fields. The trade-off between ordinary kriging and more sophisticated methods is that the latter usually imply a greater number of parameters to

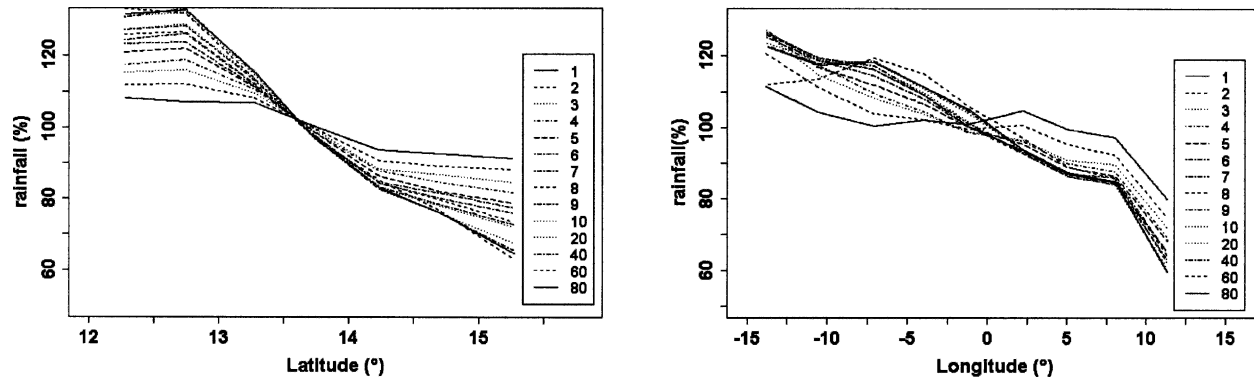


FIG. 4. The drift along progressive time scales. Each curve represents the conditional (on nonzero values) mean rainfall for the cumulative number of rainy days by band, normalized by the corresponding overall mean rainfall. The bands are either of width  $0.5^\circ$  in latitude or  $1^\circ$  in longitude. We can note a progressive augmentation of the rainfall gradient with an increasing number of rainy days, in both (left) latitude and (right) longitude. The drift exists at all of the cumulative time scales, though the gradient is smallest at the 1-day scale. The gradient is stronger as a function of latitude (from around 6% at the 1-day scale to 23% for 80 cumulative rainy days) than as a function of longitude (from around 0.13% at the 1-day scale to 3% for 80 cumulative rainy days).

infer, which, in turn, means a lack of robustness of the estimated parameters.

The first two formulations retained for the comparison are thus two ordinary kriging methods (corresponding to a stationarity assumption, assumed to hold only at the event scale and to a lesser extent at the daily scale): 1) ordinary kriging with a simple climatological variogram (no anisotropy and no nesting), denoted OK-NAN (see appendix B for a list of this and other nonstandard abbreviations used in this paper), and 2) ordinary kriging with a nested and anisotropic mean variogram, denoted OK-NA.

Three formulations are retained for the nonstationary case, with all three using a nested and anisotropic variogram (NAV) corresponding to the main features of the empirical variograms (Fig. 3b). As already mentioned, the number of rain events varies from month to month (or from one season to another), which makes the cumulative monthly (or seasonal) rain fields inhomogeneous with respect to the underlying stochastic process. To overcome this problem, the NAV is scaled for the two first nonstationary methods (UK and RK) using the classical approach proposed by Delhomme (1978); that is, the mean variogram NAV is normalized by the mean variance. This method allows one to account for the variability of the number of events. Because kriging utilizes this normalized variogram in this case, the “true” kriging variance is obtained for a given rain field by multiplying the estimated (normalized) kriging variance by the spatial variance of the field concerned. In the application of RK, the drift is computed month by month. Also, recent analyses show that there are differences in the average rainfall pattern between the eastern and the western Sahel. As a consequence,

the drift model that is used reflects these differences. The last formulation selected for the comparison is the scaling approach, referred to hereinafter as SC. Note that the above-mentioned problem of nonhomogeneity does not arise in this scaling approach because the number of events is explicitly and directly taken into account in its formulation (Ali et al. 2003). For the regional comparison, the SC formulation was used in a simplified way by assuming that the number of events is equal to the number of rainy days, because at this scale only daily rain gauges are available.

#### b. Cross validation and criteria used for the intercomparison

A cross-validation procedure (Seaman 1983) is carried out to determine which of the five formulations under consideration can produce 1) the best interpolation and 2) the more realistic value for the associated errors. Several statistical indicators will be used to that end, referring to the work of Willmott (1984), who used five statistical criteria to evaluate the performances of various interpolation methods. The rmse is sensitive to extreme values, though this problem is attenuated in this study by the extremely large size of the samples used. It was underlined that the relationship between the correlation coefficient ( $r^2$ ) and model performance is not well defined and the magnitudes of  $r^2$  are not consistently related to the accuracy of prediction. It was suggested that, in conclusion, the rmse and mean bias error (ME) are among the “best” overall measures of model performance for intercomparison.

The ME and the rmse will thus be used here as indicators of the overall coherency between the fields under comparison. Defining  $e_i$  as the difference be-

tween the estimated value  $P_i^*$  and the observed value of rainfall  $P_i$ ,

$$e_i = (P_i^* - P_i). \quad (16)$$

The mean error is

$$\text{ME} = \frac{1}{N} \sum_{i=1}^N (e_i), \quad (17)$$

with

$$N = N_s N_f, \quad (18)$$

where  $N_s$  is the number of stations (cross validation) and  $N_f$  is the number of fields. As an example, for the 8 yr of the CILSS network and a monthly time step,  $N_s = 600\text{--}650$  and  $N_f = 24$  ( $8 \times 3$ ), so that  $N \cong 15\,000$ .

The rmse is computed as

$$\text{rmse} = \left[ \frac{1}{N} \sum_{i=1}^N (e_i)^2 \right]^{1/2}. \quad (19)$$

The rmse is of special interest to this study because it provides a mean value of the estimation error that can be directly compared with the average of the theoretical standard deviation of the kriging estimation error (ksd). This rmse is considered to be the *observed error*.

Two additional criteria are computed to quantify how close the theoretical errors are to the empirical errors. The first, denoted  $I$ , is the quadratic mean of the relative errors:

$$I = \left[ \frac{1}{N} \sum_{i=1}^N \left( \frac{e_i}{\text{ksd}_i} \right)^2 \right]^{1/2}. \quad (20)$$

The closer to 1 that  $I$  is, the better the agreement is between the empirical error and the kriging theoretical error. The other additional criterion is a comparative measure of the dispersion of the theoretical error and the dispersion of the empirical errors:

$$\begin{aligned} P_1 &= \text{Nb}(-\text{ksd}_i < e_i < \text{ksd}_i; i = 1, N) \quad \text{and} \\ P_2 &= \text{Nb}(-2 \times \text{ksd}_i < e_i < 2 \times \text{ksd}_i; i = 1, N), \end{aligned} \quad (21)$$

where Nb means “number of times that.”

### c. Results of the intercomparison

The intercomparison is carried out for the two scales covered by the two available networks: the mesoscale and the regional scale. At the mesoscale (E-N network), a direct determination of the number of rain events is possible, with the drawback being that the area covered is small in comparison to both the correlation distance of the rainfall process and the resolution of the satellite products (typically  $2.5^\circ \times 2.5^\circ$ ). The regional scale (CILSS network) is more relevant in the

perspective of satellite product validation, and the integral range of the process is well covered, with the drawback being that only daily values are available.

At the mesoscale, all three nonstationary methods provide similar and realistic values of the estimation error, provided that the variance of the point series is used as an estimate of integral range of the variogram, instead of using the empirical spatial variance computed from the observations. As already underlined by Guillot and Lebel (1999), this variance largely underestimates the variance of the process, and the theoretical errors largely underestimate the observed errors of the cross-validation procedure. At the monthly time step, the value of  $I$  is 1.02 for SC, 1.08 for RK, and 1.09 for climatological UK. These results mean that, with a direct and precise quantification of the number of rain events, SC is the method providing the best evaluation of the estimation errors, whereas RK and UK tend to underestimate slightly the estimation errors.

The second step of the intercomparison procedure is to work at the regional scale. Table 1 provides a synthesis of the results obtained for the four time steps considered and the various statistical criteria. Differences in these statistical criteria are significant because of the size of the samples (8 yr of data and cross validation on 600–650 stations, on average). There are three main results: 1) even though ME and rmse for RK are the smallest, the rmse of the different methods are generally very similar, meaning that the CILSS network is dense enough<sup>2</sup> for every kriging estimate to perform similarly in terms of interpolation [Vicente-Serrano et al. (2003) also find that RK performs a little better in their intercomparison of interpolation methods applied to annual precipitation in Spain]; 2) the theoretical estimation error is far more sensitive to the approach under consideration, with, for a given time step, differences of more than 60% in the average ksd and differences of more than 100% in the values of  $I$ ; and 3) the RK method provides the best estimates of the errors, with  $I$  being close to 1 and ksd and rmse differing by less than 5%. One obvious reason for the good behavior of RK is that the drift and the variogram of the residuals are inferred separately, because of the large size of the multiannual dataset. Another reason to con-

<sup>2</sup> A test, carried out by reducing gradually the number of stations of the network considered, showed that the differences between the results of the various methods become very significant when the number of stations is lower than 100. For the synoptic network (80 stations), the RK error becomes 55.4 mm (an increase of 1.5 mm with respect to the 600-station network) and the UK error becomes 70 mm, which is an increase of 16 mm with respect to the 600-station network. For a 25-station network the errors become 61 mm for RK and 124 mm for UK.

TABLE 1. Intercomparison of interpolation methods at the regional scale. Regression kriging performs the best, with rmse close to ksd and a value of  $I$  that is nearest to 1 at all time scales. The other methods strongly underestimate the observed errors ( $\text{ksd} < \text{rmse}$ , and  $I \gg 1$ ).

		Mean (observed)	Std dev (observed)	ME (mm)	Ksd (mm)	Rmse (mm)	$I$	$P$
Daily scale	OK-NAN climatological variogram	15.66	17.01	0.015	7.75	11.08	2.21	0.78
	OK-NA mean variogram			0.008	10.02	10.62	1.40	0.84
	RK			0.002	10.1	9.63	1.01	0.85
10-day scale	UK	53.94	43.27	0.05	25.72	29.73	1.26	0.72
	SC			-0.10	21.47	28.38	1.13	0.61
	RK			0.02	26.82	26.98	1.01	0.74
Monthly scale	UK	158.60	103.17	0.08	33.69	54.11	1.61	0.56
	SC			0.10	37.15	54.62	1.41	0.60
	RK			0.06	52.33	53.92	1.07	0.73
Annual scale	UK	493.42	208.12	0.33	77.62	99.39	1.28	0.65
	SC			0.52	64.93	101.04	1.50	0.57
	RK			0.212	101.02	101.23	1.006	0.76

sider is the fact that the residuals are more Gaussian than the raw values, because linear kriging performs best for multi-Gaussian processes. A multivariate Shapiro–Wilk normality test (Royston 1982) applied to raw monthly data of the 130 rain gauges (which have full data since 1950) was rejected. When a simple Shapiro–Wilk normality test is applied gauge by gauge and month by month (July, August, September), the test was accepted for 35% of the samples, at the level 0.1. When subtracting the drift (inferred by a generalized least squares method), the test was accepted for 82% of the gauges at the same level.

The scale-invariance method does not perform as

well as expected, which is obviously linked to the algorithm used to estimate the number of events from the number of rainy days. A not-surprising though important conclusion arising from Table 1 is the fact that using an inadequate structure function leads to unrealistic theoretical values of the estimation errors, strongly underestimating the observed errors. This is illustrated in Fig. 5, reporting the distribution of the ME values at the monthly scale on the left and the distribution of the ksd values on the right. Caution is thus required when using a kriging error directly as an estimate of the ground-based error in the evaluation of satellite algorithms.

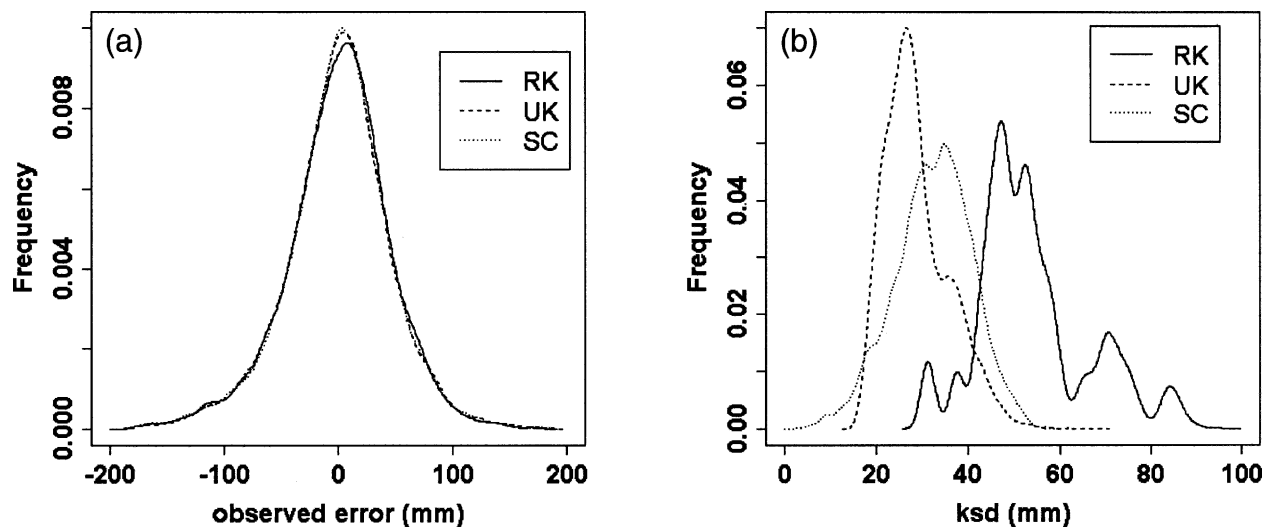


FIG. 5. (a) Distributions of the observed errors obtained by three different kriging estimates, computed by a cross-validation procedure over the 600–650 observations available each month (Jul, Aug, Sep) of an 8-yr period. (b) Distributions of the theoretical kriging standard deviations computed with the same four methods. The kriging interpolation value is not significantly different, as shown in (a); in contrast, the kriging estimation variance is more sensitive to the method under consideration, as shown in (b).

### 5. Adaptation of the scaling approach and derivation of the error function

The intercomparison of the various kriging formulations presented in section 4 was carried out through a cross-validation procedure comparing measured and reconstituted point values. Most users are interested rather in evaluating the error associated with an areal estimation. This is especially true when it comes to the evaluation of satellite estimates computed over grid cells of typical size  $1^\circ \times 1^\circ$  or  $2.5^\circ \times 2.5^\circ$ . In many circumstances, most linear interpolators that take the geometry of the measurement network into account (which is not the case for the arithmetic mean) produce similar results (Weber and Englund 1992). In our case, this is clear from the results of Table 1. Differences in rmse of point interpolation are small, and they would be still smaller for areal values (because there are no "observed" areal values, the intercomparison of section 4 cannot be carried out for areal estimates) given the smoothing out of errors produced by spatial averaging. On the other hand, using a nonoptimal method generates unrealistically low theoretical errors, as shown in section 4. Based on this, Lebel and Amani (1999) derived an error function analytically that could be applied to evaluate the errors associated with areal rainfall estimation independent of the estimation method used, providing that it makes a reasonable use of the information available on the structure of the phenomenon. This method is based on the time-scaling properties of the rain fields and was successfully validated at the mesoscale. The general expression of the function giving the *relative* error is the following:

$$e(A, N_g, K_T, P_T) = \frac{C_1}{\sqrt{N_g} \sqrt{K_T}} \left( \frac{P_T}{K_T} \right)^{-0.2} \times \left[ C_2 + C_3 \log \left( \frac{A}{N_g} \right) \right] + C_4, \quad (22)$$

where  $A$  is the area ( $\text{km}^2$ ) for which the estimation is performed,  $N_g$  is the number of gauges over this area,  $K_T$  and  $P_T$  are the number of rain events and rainfall total, respectively, over the period considered, and  $C_1$ ,  $C_2$ ,  $C_3$ , and  $C_4$  are parameters whose values may depend on the area  $A$  considered.

Rather than providing standard errors for 10-day or monthly rainfall estimates, this error function yields the error associated with the estimation of a  $P_T$  cumulative rainfall produced by  $K_T$  rain events. As seen in section 4, the direct application of the scaling approach at the regional scale does not perform so well, which is likely

to be due to a poor evaluation of the number of rain events (it was shown that SC was the best method at the mesoscale when the number of rain events was directly and precisely quantified). Following a procedure presented in Ali (2004), the SC method was thus adapted to handle situations in which only daily data are available. The resulting values taken by the parameters  $C_1$ ,  $C_2$ ,  $C_3$ , and  $C_4$  of Eq. (22) are as follows. For a  $1^\circ \times 1^\circ$  grid cell,  $C_1 = 1.05$ ,  $C_2 = 0.25$ ,  $C_3 = 0.11$ , and  $C_4 = 0.03$ , which leads to

$$e(A, N_g, K_T, P_T) = \frac{1.05}{\sqrt{N_g} \sqrt{K_T}} \left( \frac{P_T}{K_T} \right)^{-0.2} \times \left[ 0.25 + 0.11 \log \left( \frac{A}{N_g} \right) \right] + 0.03. \quad (23a)$$

For a  $2.5^\circ \times 2.5^\circ$  grid cell,  $C_1 = 1.05$ ,  $C_2 = 0.28$ ,  $C_3 = 0.17$ , and  $C_4 = 0$ , which leads to

$$e(A, N_g, K_T, P_T) = \frac{1.05}{\sqrt{N_g} \sqrt{K_T}} \left( \frac{P_T}{K_T} \right)^{-0.2} \times \left[ 0.28 + 0.17 \log \left( \frac{A}{N_g} \right) \right]. \quad (23b)$$

The distribution of errors obtained with these two error functions is close to the corresponding reference RK distributions of errors (Fig. 6). The error function [Eqs. (23a) and (23b)] can thus be used as a realistic approximation to compute the uncertainty of areal rainfall estimation in this region. One factor that is not explicitly accounted for in this formula is the spatial distribution of the gauges inside the cell of interest. However, because the parameters  $C_2$  and  $C_3$  were optimized using the current Sahelian network, their values implicitly incorporate the diversity of situations ranging from an almost uniform distribution in some cells to much more uneven distributions in other cells.

Typical error values for average months of September and August are given in Table 2. Figure 7 shows how the estimation error for a cumulative rainfall of 210 mm (average August rainfall) decreases when the number of stations increases, depending on the number of events. For instance, on a  $2.5^\circ \times 2.5^\circ$  cell, a similar error of about 15% is obtained for the four following configurations: 5 events–7 stations, 10 events–5 stations, 15 events–4 stations, and 25 events–3 stations. Another result worth noting in Table 2 stems from the comparison of the errors computed for one station on a  $1^\circ \times 1^\circ$  cell with those computed for six stations on a

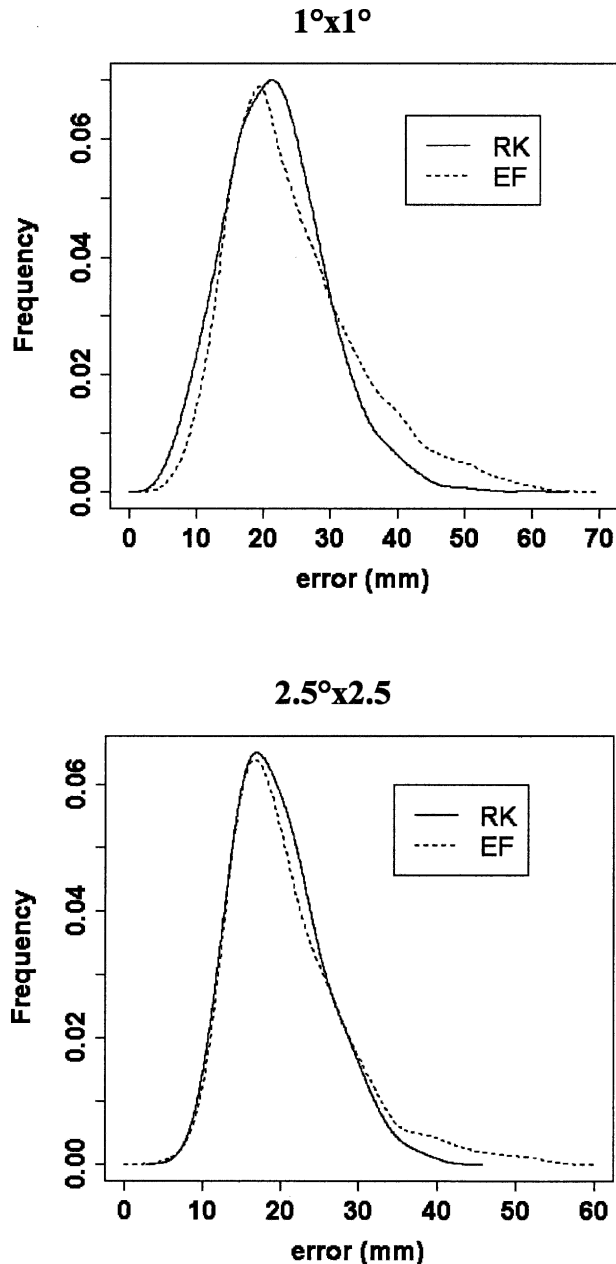


FIG. 6. Comparison of the distribution of errors obtained with the error function [Eqs. (23)] and with a full application of the reference kriging algorithm (regression kriging). The errors are computed over the 6720  $1^\circ \times 1^\circ$  and the 1152  $2.5^\circ \times 2.5^\circ$  cells covered by the CILSS network. The two distributions are very similar. However, for the  $1^\circ \times 1^\circ$  cells, the error function tends to overestimate slightly the frequency of the larger errors (between 35 and 60 mm).

$2.5^\circ \times 2.5^\circ$  cell (italicized numbers in Table 2). These two configurations correspond to approximately the same density of observations. However, the errors are far smaller for six stations on a  $2.5^\circ \times 2.5^\circ$  cell than for one station on a  $1^\circ \times 1^\circ$  cell; the spatial integration over

TABLE 2. Estimation errors (%) for average months of Aug (210 mm in 15 events) and Sep (70 mm in 6 events)—climatological values for the region of Niamey. See text for explanation of italicized numbers.

		1 station	3 stations	6 stations	10 stations
Aug	$1^\circ \times 1^\circ$	23.5	13.7	10.1	8.2
	$2.5^\circ \times 2.5^\circ$	35	18.5	<i>12.3</i>	9.1
Sep	$1^\circ \times 1^\circ$	36.6	20.6	14.6	11.5
	$2.5^\circ \times 2.5^\circ$	57.3	30.3	<i>20.1</i>	14.9

large areas significantly reduces the effect of the variability of the phenomenon.

Equations (23) take into account the time structure of rainfall through the parameter  $K_T$  and will thus in general provide more accurate values of the estimation errors than do methods that do not take into account this time structure. A simplified climatological formulation considers that all of the rain events bring the same amount of point rainfall  $m_e$ , meaning that when  $P_T$  is known then  $K_T = P_T/m_e$ . Assuming this mean event rain depth  $m_e$  to be 14 mm (as determined from the E-N observations), then Eq. (23a) may be written as

$$e(A, N_g, K_T, P_T) = \frac{1.05\sqrt{14}}{\sqrt{N_g}\sqrt{P_T}} (14)^{-0.2} \times \left[ 0.25 + 0.11 \log\left(\frac{A}{N_g}\right) \right] + 0.03.$$

Replacing  $A$  by its value for a  $1^\circ \times 1^\circ$  cell (12 000 km<sup>2</sup>), it then becomes

$$e(N_g, P_T)_{1^\circ} = \frac{0.232}{\sqrt{N_g}\sqrt{P_T}} [1.28 - 0.11 \log(N_g)] + 0.03. \quad (24a)$$

In a similar way, for a  $2.5^\circ \times 2.5^\circ$  cell (75 000 km<sup>2</sup>),

$$e(N_g, P_T)_{2.5^\circ} = \frac{0.232}{\sqrt{N_g}\sqrt{P_T}} [2.19 - 0.17 \log(N_g)]. \quad (24b)$$

The errors computed using the climatological formula in Eqs. (24) are reported in Fig. 7 (thick dashed line) for the month of August (15 events bringing 14 mm each), showing that, in the case of rain events that are stronger than average (meaning a smaller number of events), using the climatological formula leads to a significant underestimation of the estimation error. In reality, the most common situation is when one or two very strong events occur. This will not necessarily change by much the total number of rain events, but it will produce a similar effect to having a smaller number

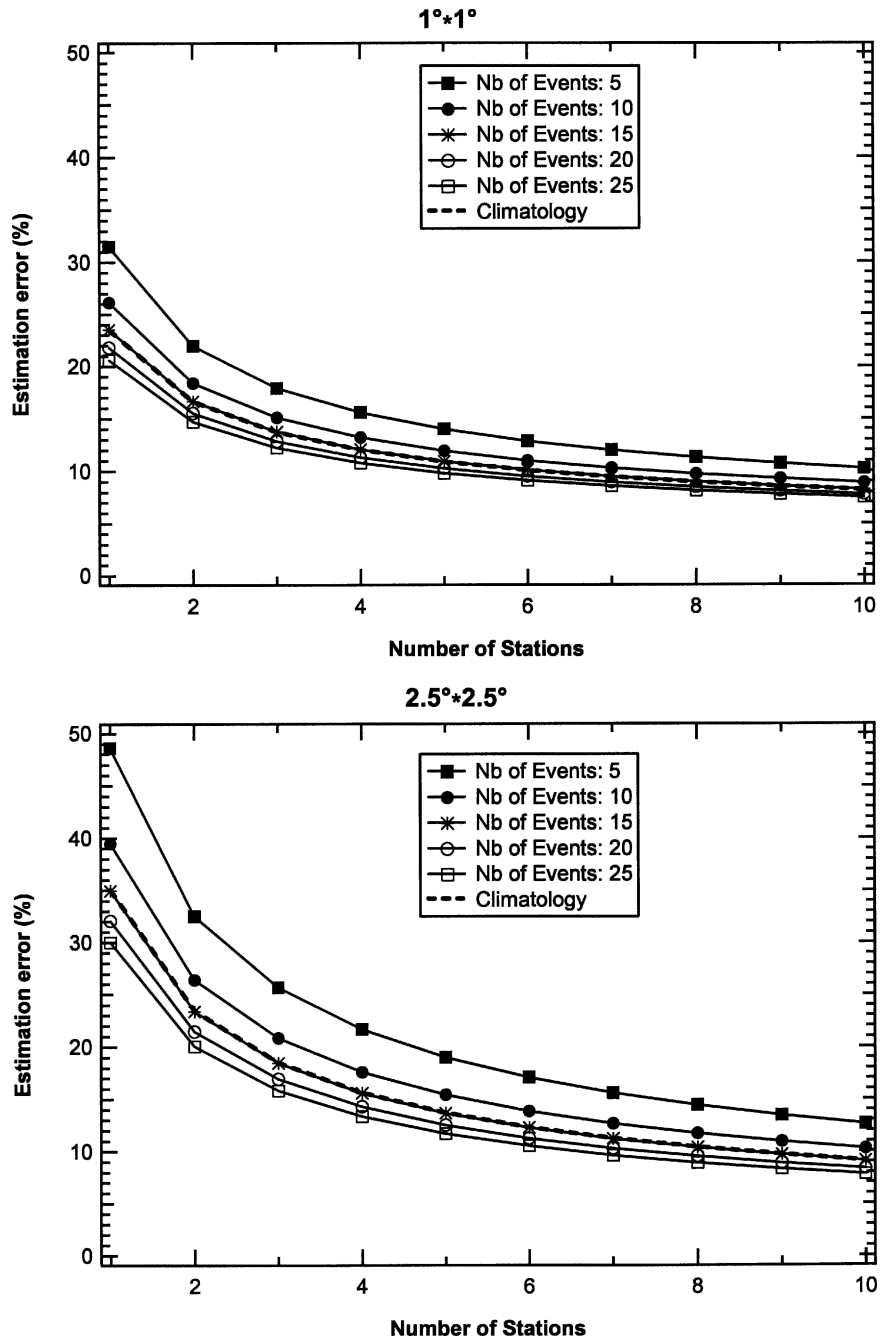


FIG. 7. Estimation error (for an Aug mean rainfall of 210 mm) as a function of the number of available stations; the errors are computed using the error functions in Eq. (23a) ( $1^\circ \times 1^\circ$ ) and Eq. (23b) ( $2.5^\circ \times 2.5^\circ$ ) for different time distributions of the monthly rainfall (the time distribution is represented by the number of events  $K_T$  having produced the monthly total of 210 mm). The simplified formulas correspond to a mean event rainfall of 14 mm, or 15 events for a monthly rainfall of 210 mm [Eqs. (24a) and (24b)].

of events because there will be a large error associated with the strong events [this effect was studied in Lebel and Amani (1999)].

In Fig. 8 the errors obtained for the three most rainy

months (July, August, September) with the climatological formula are compared. If one considers the average situation of three stations on a  $1^\circ \times 1^\circ$  cell and 15 stations on a  $2.5^\circ \times 2.5^\circ$  cell, then the climatological

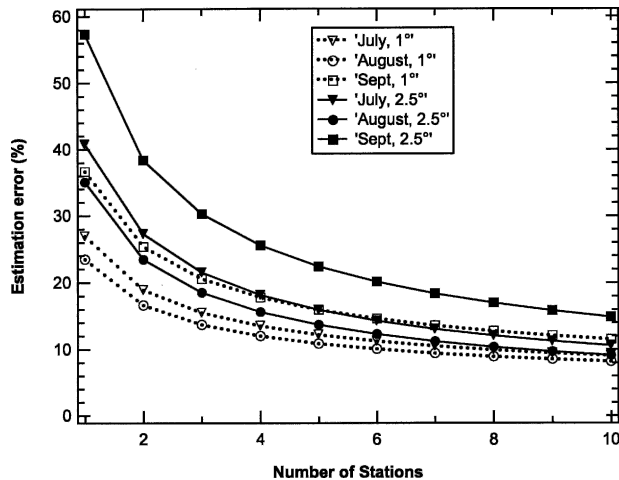


FIG. 8. Estimation errors for the three most rainy months (Jul, Aug, Sep). The errors are computed for the average monthly rainfall and number of events of the period 1990–2000 in the region of Niamey (Jul: 155 mm in 11 major events; Aug: 210 mm in 15 major events; Sep: 70 mm in 6 major events).

errors range from 14% to 20% on the  $1^\circ \times 1^\circ$  cell and from 7% to 12% on the  $2.5^\circ \times 2.5^\circ$  cell. With a more favorable—but much less representative of the average situation—density of six stations on a  $1^\circ \times 1^\circ$  cell, the climatological errors decrease to 10% in August and 14% in September. Note that, after correction for different densities and area of integration, these values remain larger by about 15%–20% than those computed in Lebel and Amani (1999) for an area of 10 000 km<sup>2</sup>. For instance, Lebel and Amani (1999) gave an error of 9% for a four-station network on 10 000 km<sup>2</sup>, as compared with 10.8% computed here with Eq. (24) for a five-station network on a  $1^\circ \times 1^\circ$  cell (11 800 km<sup>2</sup>). This is due to the second nested structure in the variogram that was neglected in Lebel and Amani (1999).

## 6. Conclusions

The ultimate goal of the work presented here was to develop and validate an error function to be used as a tool in the evaluation of the performances of satellite rainfall products over the Sahel. This development was carried out in three steps, each of which produced its own results.

The first step led to the identification of the average structure of the Sahelian rain fields at five time steps (rain event, daily, 10 day, monthly, and seasonal). These fields are all characterized by a strong anisotropy and, for time steps larger than daily, are spatially non-stationary. It is therefore necessary to identify the climatological drift before inferring the structure function

of the stationary residuals to the drift. This structure function is made of two nested structures. The first corresponds to the convective scale. The decorrelation distance ( $0.2^\circ$ ) and anisotropy coefficient (0.5) are invariant with the time step considered. The second structure is related to the general organization of the mesoscale convective systems and is characterized by a decorrelation distance increasing from  $4^\circ$  for daily rainfall to  $5^\circ$  for annual rainfall. The anisotropy (0.3) coefficient is larger than the anisotropy coefficient of the first structure.

The second step used two networks representing different scales (E-N, 16 000 km<sup>2</sup>; CILSS,  $3 \times 10^6$  km<sup>2</sup>) to intercompare five kriging algorithms, whose optimality depends on the relevance of the structure function used. At the regional scale more than 600 rain gauges were available to carry out a cross-validation study focusing on 3 months (July, August, September) and 8 yr. All methods perform similarly in terms of estimation bias with an average error of 54 mm at the monthly scale, for instance. Regression kriging appears to be the best method in the sense that its theoretical errors are the closest to the observed errors, as computed from the cross-validation procedure. The superiority of regression kriging is attributed both to an accurate representation of the drift and to the residuals being more Gaussian in distribution than the raw values are.

The last step was the derivation of an error function to be applied for computing relevant estimation errors when rainfall is estimated over grid cells (in the previous step, the cross validation relates to the estimation of point values). The analytical formulation allows the computation of the error associated with rainfall estimation over an area  $A$  with a number  $N_g$  of gauges over this area. For the CILSS network—the best network possibly accessible today in the region—80% of the monthly estimation errors over the 280  $1^\circ \times 1^\circ$  cells of the region range from 8% to 28% and 80% of the monthly estimation errors over the 48  $2.5^\circ \times 2.5^\circ$  cells of the region range from 5% to 22%. Typical errors for the average situation of three stations on a  $1^\circ \times 1^\circ$  cell and 15 stations on a  $2.5^\circ \times 2.5^\circ$  cell were also computed. The climatological errors range from 14% for the month of August to 20% for the month of September on the  $1^\circ \times 1^\circ$  cell and from 7% for the month of August to 12% for the month of September on the  $2.5^\circ \times 2.5^\circ$  cell. The theoretical errors given here, taking into account the anisotropy and nested structure of the Sahelian rain fields and extensively validated on observations using a cross-validation procedure, are deemed to be more accurate than those previously computed by Lebel and Amani (1999).

The logical follow up of this work—that is, using the

TABLE A1. Parameters of the variograms inferred from the E-N and CILSS datasets. Note that the first structure is very stable at all time steps ( $S_1 = 0.2$  and  $\alpha_1 = 0.5$  or  $0.6$ ).

Spatial scale	Temporal scale	Exponential nested and anisotropic model parameters [ $\sigma_0$ : nugget, $\sigma_1$ : sill first structure, $\sigma_2$ : sill second structure (mm <sup>2</sup> ), $S_1$ : range first structure, $S_2$ : range second structure (km), and $\alpha_1$ and $\alpha_2$ : anisotropy coefficients]
Mesoscale (E-N)	Event	$\sigma_0 = 0, \sigma_1 = 100, \sigma_2 = 105, S_1 = 0.2, S_2 = 2, \alpha_1 = 0.6, \alpha_2 = 0.5$
	10-day	$\sigma_0 = 20, \sigma_1 = 380, \sigma_2 = 500, S_1 = 0.2, S_2 = 3, \alpha_1 = 0.5, \alpha_2 = 0.6$
	Monthly	$\sigma_0 = 60, \sigma_1 = 1200, \sigma_2 = 900, S_1 = 0.2, S_2 = 3.5, \alpha_1 = 0.5, \alpha_2 = 0.52$
	Annual	$\sigma_0 = 300, \sigma_1 = 3000, \sigma_2 = 4000, S_1 = 0.2, S_2 = 3.5, \alpha_1 = 0.5, \alpha_2 = 0.52$
Regional Scale (CILSS)	Day	$\sigma_0 = 0, \sigma_1 = 100, \sigma_2 = 50, S_1 = 0.2, S_2 = 4, \alpha_1 = 0.6, \alpha_2 = 0.3$
	10-day	$\sigma_0 = 210, \sigma_1 = 525, \sigma_2 = 420, S_1 = 0.2, S_2 = 4.3, \alpha_1 = 0.5, \alpha_2 = 0.3$
	Monthly	$\sigma_0 = 560, \sigma_1 = 1120, \sigma_2 = 1120, S_1 = 0.2, S_2 = 5, \alpha_1 = 0.5, \alpha_2 = 0.3$
	Annual	$\sigma_0 = 2700, \sigma_1 = 3600, \sigma_2 = 3600, S_1 = 0.2, S_2 = 5, \alpha_1 = 0.5, \alpha_2 = 0.3$

error function for the intercomparison of satellite rainfall products—is the object of a companion paper (Ali et al. 2005).

*Acknowledgments.* This research was funded by IRD and INSU in the framework of the AMMA-CATCH “ORE” program initiated by the French Ministry of Research. Special thanks are given to the Departement Soutien et Formation of IRD for the grant allocated to the first author of this paper. We also acknowledge S. Bonaventure for his efforts in the exploitation of the AGRHYMET Center rainfall database and J.-L. Diasso and J. Nicol for their help in proofreading the article.

APPENDIX A

**On the Different Variogram Models Used for Different Times Scales**

All variograms apply to the residuals ( $\varepsilon$ ) from the drift ( $m$ ), apart from the event and daily variograms. They all have the same form:

$$\gamma(h) = \sigma_0 + \sigma_1 \left[ 1 - \exp\left(-\frac{h}{S_1}\right) \right] + \sigma_2 \left[ 1 - \exp\left(-\frac{h}{S_2}\right) \right]. \tag{A1}$$

The two main axes of anisotropy are oriented east–west (EW) and south–north (SN). The anisotropy is accounted for by computing a non-Euclidian distance, using the following formula:

$$h^2 = \left[ h^2_{EW} + \left( \frac{h_{SN}}{\alpha} \right)^2 \right]^{1/2}, \tag{A2}$$

where  $\alpha$  is the anisotropy coefficient.

The parameters of the variograms inferred from the E-N and CILSS datasets are reported in Table A1.

APPENDIX B

**Some Nonstandard Notation Used in the Text**

- OK-NAN Ordinary kriging with a simple climatological variogram (no anisotropy and no nesting)
- OK-NA Ordinary kriging with a nested and anisotropic mean variogram denoted
- NAV Nested and anisotropic variogram
- Ksd The theoretical standard deviation of the kriging estimation error
- I Quadratic mean of the relative errors
- SC “Scaling” kriging

REFERENCES

Ahmed, S., and G. de Marsily, 1987: Comparison of geostatistical methods for estimating transmissivity using data on transmissivity and specific capacity. *Water Resour. Res.*, **23**, 1717–1737.

Ali, A., 2004: Modeling the scale invariance of Sahelian rain fields. Application to estimation algorithms and climatic variability studies. Ph.D. thesis, INPG Grenoble, 180 pp.

—, T. Lebel, and A. Amani, 2003: Invariance in the spatial structure of Sahelian rain fields at climatological scales. *J. Hydrometeor.*, **4**, 996–1011.

—, A. Amani, A. Diedhiou, and T. Lebel, 2005: Rainfall estimation in the Sahel. Part II: Evaluation of rain gauge networks in the CILSS countries and objective intercomparison of rainfall products. *J. Appl. Meteor.*, **44**, 1707–1722.

Boussières, N., and W. Hogg, 1989: The objective analysis of daily rainfall by distance weighting schemes on a mesoscale grid. *Atmos.–Ocean*, **27**, 521–541.

Chica-Olmo, M., and J. A. Luque-Espinar, 2002: Application of the local estimation of the probability distribution function in environmental sciences by kriging methods. *Inverse Probl.*, **18**, 25–36.

Chilès, J., and P. Delfiner, 1999: *Geostatistics: Modeling Spatial Uncertainty*. John Wiley and Sons, 695 pp.

Collins, F. C., and P. V. Bolstad, 1996: A comparison of spatial interpolation techniques in temperature estimation. *NCGIA Third Int. Conf./Workshop on Integrating GIS and Environmental Modeling*, Santa Fe, NM, National Center for Geo-

- graphical Information and Analysis, CD-ROM. [Available online at [http://www.ncgia.ucsb.edu/conf/SANTA\\_FE\\_CD-ROM/sf\\_papers/collins\\_fred/collins.html](http://www.ncgia.ucsb.edu/conf/SANTA_FE_CD-ROM/sf_papers/collins_fred/collins.html).]
- Cressie, N. A. C., 1993: *Statistics for Spatial Data*. rev. ed. John Wiley and Sons, 900 pp.
- Creutin, J. D., and C. Obled, 1982: Objective analysis and mapping techniques for rainfall fields: An objective comparison. *Water Resour. Res.*, **18**, 413–431.
- D'Amato, N., and T. Lebel, 1998: On the characteristics of rainfall events in the Sahel, with a view to the analysis of climatic variability. *Int. J. Climatol.*, **18**, 955–974.
- Delhomme, J. P., 1978: Kriging in hydrosocieties. *Water Resour.*, **1**, 251–266.
- Ecker, M. D., and A. E. Gelfand, 2003: Spatial modeling and prediction under range anisotropy. *Environ. Ecol. Stat.*, **10**, 165–178.
- Furrer, R., 2002: Aspects of modern geostatistics: Nonstationarity, covariance estimation and state-space decompositions. Ph.D. thesis, Federal Institute of Technology in Lausanne, 139 pp.
- Gandin, L. S., 1965: *Objective Analysis of Meteorological Fields* (translated from Russian by R. Hardin). Israel Program for Scientific Translation, 242 pp.
- Goovaerts, P., 1997: *Geostatistics for Natural Resources Evaluation*. Oxford University Press, 483 pp.
- Guillot, G., and T. Lebel, 1999: Approximation of Sahelian rainfall fields with meta-Gaussian random functions. Part 2: Parameter estimation and comparison to data. *Stochastic Environ. Res. Risk Assess.*, **13**, 113–130.
- Hengl, T., G. B. M. Geuvelink, and A. Stein, 2003: Comparison of kriging with external drift and regressing kriging. ITC Tech. Note, 18 pp. [Available online at [http://www.itc.nl/library/Academic\\_output/](http://www.itc.nl/library/Academic_output/).]
- Huang, H. C., N. Cressie, and J. Gabrosek, 2002: Fast spatial prediction of global processes from satellite data. *J. Comput. Graphical Stat.*, **11**, 63–88.
- Huff, F. A., 1970: Sampling errors in measurement of mean precipitation. *J. Appl. Meteor.*, **9**, 35–44.
- Huffman, G. J., 1997: Estimation of root-mean-square random error for finite samples of estimated precipitation. *J. Appl. Meteor.*, **36**, 1191–1201.
- Journel, A. G., 1983: Nonparametric estimation of spatial distributions. *Math. Geol.*, **15**, 445–468.
- , and C. J. Huijbregts, 1978: *Mining Geostatistics*. Academic Press, 597 pp.
- Lebel, T., and A. Amani, 1999: Rainfall estimation in the Sahel: What is the ground truth? *J. Appl. Meteor.*, **38**, 555–568.
- , G. Bastin, C. Obled, and J. D. Creutin, 1987: On the accuracy of areal rainfall estimation: A case study. *Water Resour. Res.*, **23**, 2123–2134.
- , A. Diedhiou, and H. Laurent, 2003: Seasonal cycle and interannual variability of the Sahelian rainfall at hydrological scales. *J. Geophys. Res.*, **108**, 8389, doi:10.1029/2001JD001580.
- Matheron, G., 1969: Le krigeage universel (Universal kriging). Ecole des Mines de Paris, Cahiers du Centre de Morphologie Mathématique de Fontainebleau, Fasc. 1, 83 pp.
- , 1971: The theory of regionalised variables and its applications. Ecole des Mines de Paris, Cahiers du Centre de Morphologie Mathématique de Fontainebleau, Fasc. 5, 211 pp.
- , 1976: A simple substitute for conditional expectation: The disjunctive kriging. *Advanced Geostatistics in the Mining Industry*, M. Guarascio, M. David, and C. J. Huijbregts, Eds., Reidel, 221–236.
- Moyeed, R. A., and A. Papritz, 2002: An empirical comparison of kriging methods for nonlinear spatial point prediction. *Math. Geol.*, **34**, 365–386.
- Odeh, I., A. McBratney, and D. Chittleborough, 1995: Further results on prediction of soil properties from terrain attributes: Heterotopic cokriging and regression-kriging. *Geoderma*, **67**, 215–226.
- Papritz, A., and A. Stein, 1999: Spatial prediction by linear kriging. *Spatial Statistics for Remote Sensing*, A. Stein, F. Van der Meer, and B. Gorte, Eds., Kluwer Academic, 83–113.
- Philips, R. H., J. Dolph, and D. Marks, 1992: A comparison of geostatistical procedures for spatial analysis of precipitation in mountainous terrain. *Agric. For. Meteorol.*, **58**, 119–141.
- Rivoirard, J., 1994. *Introduction to Disjunctive and Non-Linear Geostatistics*. Oxford University Press, 181 pp.
- Royston, P., 1982: An extension of Shapiro and Wilk's *W* test for normality to large samples. *Appl. Stat.*, **31**, 115–124.
- Rudolf, B., H. Hauschild, W. Rueth, and U. Schneider, 1994: Terrestrial precipitation analysis: Operational methods and required density of point measurements. *Global Precipitation and Climate Change*, M. Desbois and F. Desalmand, Eds., NATO ASI Series, Vol. 1, Springer-Verlag, 173–186.
- Sampson, P., and P. Guttorp, 1992: Nonparametric estimation of nonstationary spatial covariance structure. *J. Amer. Stat. Assoc.*, **87**, 108–119.
- Seaman, R. S., 1983: Objective analysis accuracies of statistical interpolation and successive correction schemes. *Aust. Meteor. Mag.*, **31**, 225–240.
- Vicente-Serrano, S. M., M. A. Saz-Sanchez, and J. M. Cuadrat, 2003: Comparative analysis of interpolation methods in the middle Ebro Valley (Spain): Application to annual precipitation and temperature. *Climate Res.*, **24**, 161–180.
- Wackernagel, H., 1998: *Multivariate Geostatistics: An Introduction with Applications*. 2d ed. Springer-Verlag, 291 pp.
- Weber, D. D., and E. J. Englund, 1992: Evaluation and comparison of spatial interpolators. *Math. Geol.*, **24**, 381–391.
- Willmott, C. J., 1984: On the evaluation of model performance in physical geography. *Spatial Statistics and Models*, G. L. Galle and C. J. Willmott, Eds., D. Reidel, 443–460.
- Zimmerman, D. L., C. Pavlik, A. Ruggles, and M. P. Armstrong, 1999: An experimental comparison of ordinary and universal kriging and inverse distance weighting. *Math. Geol.*, **31**, 375–390.